



Enhancing the Reliability and Throughput of Neurosphere Culture on Hydrogel Microwell Arrays

Journal:	<i>Stem Cells</i>
Manuscript ID:	SC-08-0498.R1
Manuscript Type:	Original Research
Date Submitted by the Author:	n/a
Complete List of Authors:	Cordey, Myriam; Ecole Polytechnique Fédérale de Lausanne (EPFL) Limacher, Monika; Ecole Polytechnique Fédérale de Lausanne (EPFL) Kobel, Stefan; Ecole Polytechnique Fédérale de Lausanne (EPFL) Taylor, Verdon; Max Planck Institute of Immunobiology Lutolf, Matthias; Ecole Polytechnique Fédérale de Lausanne (EPFL)
Keywords:	Clonal assays, Experimental models, Microarray, Neural stem cell, Stem cell culture, Stem/progenitor cell
<p>Note: The following files were submitted by the author for peer review, but cannot be converted to PDF. You must view these files (e.g. movies) online.</p> <p>Supplementary Movie 1 R1.mov Supplementary Movie 2 R1.mov Supplementary Movie 3 R1.mov Suppl Movie V4.mp4 Suppl Movie V5.mp4</p>	



Enhancing the Reliability and Throughput of Neurosphere Culture on Hydrogel Microwell Arrays

Running title: Microarrayed Neurosphere Culture

MYRIAM CORDEY^a, MONIKA LIMACHER^a, **STEFAN KOBEL^a**, VERDON
TAYLOR^b & MATTHIAS P. LUTOLF^{a*}

^aLaboratory of Stem Cell Bioengineering, Institute of Bioengineering, Ecole Polytechnique
Fédérale de Lausanne (EPFL), Lausanne, Switzerland

^bMax Planck Institute of Immunobiology, Department of Molecular Embryology, Stübeweg 51,
D-79108 Freiburg, Germany

Author contribution summary:

Myriam Cordey: Assembly of data, data analysis and interpretation, manuscript writing

Monika Limacher: Assembly of data, data analysis and interpretation

Stefan Kobel: Assembly of data, data analysis and interpretation

Verdon Taylor: Provision of neural stem cells, data analysis and interpretation, manuscript writing

Matthias Lutolf: Conception and design, data analysis and interpretation, financial support, manuscript writing

***Correspondence:** Matthias P. Lutolf, Ph.D., Institute of Bioengineering, Laboratory of Stem Cell Bioengineering, Ecole Polytechnique Fédérale de Lausanne (EPFL), Bldg. AI 3138, Station 15, CH-1015 Lausanne, Switzerland, phone: +41 21 693 18 76, fax: +41 21 693 96 65, e-mail: matthias.lutolf@epfl.ch

Key Words. Neural stem cells • Neurospheres • Microwell arrays • Hydrogels • Cell culture • Clonal assays

1
2
3
4
5
6
7
8
9
10
11
12
13
14
15
16
17
18
19
20
21
22
23
24
25
26
27
28
29
30
31
32
33
34
35
36
37
38
39
40
41
42
43
44
45
46
47
48
49
50
51
52
53
54
55
56
57
58
59
60

Cordey et al.

ABSTRACT

The neurosphere assay is the standard retrospective assay to test the self-renewal capability and multipotency of neural stem cells (NSC) *in vitro*. However, it has recently become clear that not all neurospheres are derived from a NSC and that on conventional cell culture substrates, neurosphere motility may cause frequent neurosphere ‘merging’ (Singec *et al.*, Nature Methods, 2006; Jessberger *et al.*, Stem Cells, 2007). Combining biomimetic hydrogel matrix technology with microengineering, we developed a microwell array platform on which NSC fate and neurosphere formation can be unequivocally attributed to a single founding cell. Using time-lapse microscopy and retrospective immunostaining, the fate of several hundred single NSCs was quantified. Compared to conventional neurosphere culture methods on plastic dishes, we detected a more than 100% increase in single NSC viability on soft hydrogels. Effective confinement of single proliferating cells to microwells led to neurosphere formation of vastly different sizes, a high percentage of which showed stem cell phenotypes after one week in culture. The reliability and increased throughput of this platform should help to elucidate better the function of sphere-forming stem/progenitor cells independent of their proliferation dynamics.

INTRODUCTION

Stem cells are characterized by their dual ability to self-renew and differentiate, yielding large numbers of progeny that can form, maintain and regenerate tissues. Due to these unique properties, the therapeutic potential of stem cells is significant. However, to fully exploit this potential and enlist stem cells therapeutically, we must better understand the molecular mechanisms that govern stem cell function.

Experimental assays that can reliably identify stem cells and help exploring their function are indispensable tools to further our fundamental understanding of stem cell regulation. The paradigmatic assay of mammalian adult stem cell function is the long-term reconstitution of blood upon transplantation of hematopoietic stem cells (HSCs) into lethally irradiated recipients¹. Self-renewal of these rare, phenotypically well-characterized cells can be unambiguously defined by long-term multilineage engraftment at the single cell level and over multiple generations in serial transplantation assays. Similarly rigorous experimental paradigms have yet to be developed for most other somatic stem cells. In the absence of a functional *in vivo* assay, the definition and characterization of stem cells relies, at least to some extent, on *in vitro* assays. A case in point is the *in vitro* assessment of neural stem cell (NSC) function of the mammalian central nervous system. In serum-free medium and in the presence of mitogens such as epidermal growth factor (EGF) and/or fibroblast growth factor (FGF)-2, NSCs can be cultured on non-adhesive surfaces as multicellular spheres, termed *neurospheres*². The extensive proliferation of neurosphere-forming cells has been used as an indicator of stem cell function based on the assumption that all neurospheres are derived from a stem cell. Over the last 15 years or so, this assay has become an indispensable tool to identify

1 Cordey et al.

2
3 putative stem cells in different regions of the central nervous system in the adult and at
4
5 defined developmental stages, and has also been used to probe the perturbation of their
6
7 self-renewal and differentiation functions in response to numerous regulatory cues³.
8
9

10
11 However, just as any other *in vitro* assay, the neurosphere assay is not without its
12
13 limitations³⁻⁸. Neurosphere cultures become heterogeneous with time in culture and the
14
15 frequency of sphere-forming cells reduces to a few percent⁹. Accordingly, it may be
16
17 problematic to correlate neurosphere numbers with stem cell numbers, as neurospheres
18
19 can also form from progenitor cells^{4,8}. Thus, the neurosphere assay expands cells that
20
21 proliferate in response to defined growth factors, but not necessarily NSCs. Extensive
22
23 research on HSCs and other adult stem cells has shown that stem cells reside
24
25 predominantly in a relatively quiescent G₀ state^{10,11} and that even *in vitro*, primitive cells
26
27 may be quiescent with slower proliferation kinetics compared to more committed
28
29 progenitors¹². Importantly, neurospheres are motile and can merge with each other even
30
31 under culture conditions considered as clonal^{5,6}. **At the level of individual cells, NSCs**
32
33 **have also been observed to spontaneously fuse⁶. Although a rare event (ca. 0.2% of**
34
35 **proliferating cells) that appears to lead to cell death, cell fusion could adversely affect the**
36
37 **genetic composition of NSC cultures.**
38
39
40
41
42

43
44 Our goal was to develop an alternative to the neurosphere assay that permits *i*) to
45
46 explore neurosphere formation from single cells in the absence of sphere aggregation,
47
48 and *ii*) to capture the dynamic behavior of individual neurosphere-derived cells via time-
49
50 lapse microscopy completely independent of their proliferation kinetics. Thus one could
51
52 generate a 'snapshot' of the single cell dynamics of a given NSC population. Due to the
53
54 heterogeneity of neurosphere cultures, we targeted an assay format that would be
55
56
57
58
59
60

1
2
3 amenable to high-throughput experimentation with regards to the number of individual
4
5 stem cells tested.
6

7
8 We used standard photolithography techniques to generate microwell arrays¹³⁻¹⁵
9
10 from soft and highly hydrated poly(ethylene glycol) (PEG)-based hydrogels¹⁶. This
11
12 microengineered culture platform has proven very effective in confining single NSCs and
13
14 in guiding their extensive proliferation to form neurospheres of vastly different sizes. The
15
16 high density of microwells on the arrays allowed a simultaneous tracking of several
17
18 hundred live single cells via time-lapse microscopy, and a quantitative assessment of
19
20 their viability and proliferation kinetics. Retrospective immunostaining of neurospheres
21
22 grown within these arrays confirmed a high percentage of stem cell potential after one
23
24 week in culture on microwell arrays. This platform should serve as robust alternative to
25
26 the conventional neurosphere assay to study NSC function *in vitro*.
27
28
29
30
31
32
33
34
35
36
37
38
39
40
41
42
43
44
45
46
47
48
49
50
51
52
53
54
55
56
57
58
59
60

1 Cordey et al.

2
3 **MATERIALS AND METHODS**

4
5 **Hydrogel Precursor Synthesis**

6
7
8 Pentaerythriol tetra(mercaptoethyl) polyoxyethylene (4armPEG-thiol), (mol. wt.
9
10 40000g/mol, 98.9% substitution as indicated by manufacturer) and hexaglycerol
11
12 polyethyleneglycol ether (8arm-PEG-OH, mol. weight 10063 g/mol, $M_w/M_n = 1.1$, 99%
13
14 substitution as indicated by manufacturer) were obtained from NOF Corporation (Japan).
15
16 Divinyl sulfone was purchased from Aldrich (Buchs, Switzerland). 8arm-PEG-
17
18 vinylsulfones (8arm-PEG-VS) were produced and characterized as described elsewhere¹⁷.
19
20 The final product was dried under vacuum and stored under argon at -20°C. The product
21
22 was analyzed by gel permeation chromatography (GPC) using waters separation module
23
24 equipped with a 515 HPLC pump, a series of Styragel columns (HR2, HR3, and HR4
25
26 with pore sizes 102, 103, and 104 Å, respectively), and waters 410 differential
27
28 refractometer for detection. THF was used as eluent at a flow rate of 1 ml/min at 40°C to
29
30 confirm the identical molecular weight distribution of PEG-OH and PEG-VS. The degree
31
32 of end group conversion was 88.8 % as determined via ¹H NMR (CDCl₃) on a Bruker
33
34 (400 MHz): 3.6 ppm (PEG backbone), 6.1 ppm (d, 1H, =CH₂), 6.4 ppm (d, 1H, =CH₂),
35
36 and 6.8 ppm (dd, 1H, -SO₂CH=).

37
38
39
40
41
42
43
44
45 **Surface Modification of Glass Slides**

46
47
48 Microscopic glass slides were modified by a treatment with 3-mercaptopropyl-
49
50 trimethoxysilane (MPS) (Falcone, Switzerland) in order to expose free thiol groups that
51
52 could react with the VS-groups and covalently graft hydrogels to the glass surface. The
53
54 silanization was performed as previously described¹⁸. Briefly, the glass slides were
55
56
57
58
59
60

1
2
3 cleaned with detergent, bi-distilled water and ethanol and dried on air. In a bath of 150 ml
4
5 toluene, 1.5 ml MPS and 5 drops (~ 0.2 ml) of acetic acid was mixed for 30 min. The
6
7 glass slides were immersed for 30 min, rinsed with toluene and dried on air, followed by
8
9 a baking step of 1 hour at 110°C. Prior to usage, the slides were immersed for 10 min in
10
11 10 mM DTT solution to reduce disulfide bonds, washed with bi-distilled water and dried
12
13 on air.
14
15
16

17 18 19 20 **Formation of Thin Hydrogel Films on Glass Slides**

21
22 PEG hydrogels were formed from 8armPEG-VS and 4armPEG-thiol macromers (at 5%
23
24 v/w) as thin films on glass slides as described elsewhere¹⁷ (**Fig. 1A**). PEG-VS was
25
26 dissolved in 0.3 M triethanolamine (TEOA, Fluka, N° 90279), and 4armPEG-thiol was
27
28 dissolved in bi-distilled water. A film of defined thickness (100 µm) was prepared in a
29
30 sandwich structure using a spacer.
31
32
33

34 35 36 **Determination of Hydrogel Swelling**

37
38 Gel disks with a volume of 50µl were synthesized as described above, their weight and
39
40 density in air and ethanol before and after swelling at room temperature determined on
41
42 the basis of Archimedes' buoyancy principle¹⁷. A swelling ratio Q (=Volume of swollen
43
44 gels/Volume of dry polymer) of 22.6 +/- 1.9 was determined at 5% solid precursor
45
46 content, corresponding to a water content of approximately 96 %. Relative to the gel
47
48 volume during cross-linking, gels only swelled by a factor of 1.45 (+/- 0.02). The
49
50 minimal swelling led to stable hydrogel films that adhered to the substrate even after
51
52 storing for more than a month in water at room temperature.
53
54
55
56
57
58
59
60

Cordey et al.

Patterning of Microwell Arrays by PDMS Stamping of Soft Hydrogels

Hydrogel microwell arrays were fabricated via a multi-step soft lithography process (**Fig. 1A**). First, a topographically structured silicon wafer was fabricated, then PDMS was cast onto this structure, and finally the hydrogel films were patterned in a stamping step using this PDMS stamp. A 4-inch Silicon (Si) wafer was designed using the layout editor of CleWin. A pattern was selected consisting of 8 squares, each square matching the dimensions of a standard 96-well plate. Each square included $33 \times 33 = \sim 1'000$ wells with a diameter of $100 \mu\text{m}$ and $50 \mu\text{m}$ distance per well. The data from the CleWin program was converted and transferred to the laser-writing machine for the mask fabrication conducted in the clean room facility of EPFL. After the writing of the chrome-blank mask (Nanofilm, USA), the photoresist was developed, and chrome etched two times for 5 min before stripping off the photoresist (2×15 min). These steps resulted in a mask with transparent and non-transparent parts, which was later used for photolithography. The Si wafer was cleaned in oxygen plasma for 4 min and then spin coated (1700 rpm) with a $50 \mu\text{m}$ thick negative photoresist (GM1070, from Gersteltec, Switzerland). The coated wafer was prebaked (5 min at 130°C , $4^\circ\text{C}/\text{min}$) before exposing for 3×13 sec to UV light through the mask and postbaked (40 min at 105°C , $4^\circ\text{C}/\text{min}$). The unexposed part was washed away with PGMEA (Propylene glycol monomethyl ether acetate) for 2×2 min, cleaned with IPA (Isopropyl alcohol) and air-dried. This resulted in the desired 3D structured wafer, where the well depth was determined by the photoresist thickness of $50 \mu\text{m}$. The structured wafer was then used to mold PDMS (Sylgard[®] 184 Silicone Elastomer, Dow Corning Corporation, USA). The components

1
2
3 were mixed in a weight ratio of 10 parts of base and one part of curing agent. The PDMS
4 replicas were carefully peeled off and cut to the desired size. The hydrogel film was
5
6 fabricated as described in the previous section and, after 30 minutes of hydrogel
7
8 crosslinking, the PDMS stamps were pressed onto film. The PDMS was finally released
9
10 from the hydrogel after 90 minutes of complete crosslinking, thus achieving the 3D
11
12
13
14
15
16
17
18
19
20
21
22
23
24
25
26
27
28
29
30
31
32
33
34
35
36
37
38
39
40
41
42
43
44
45
46
47
48
49
50
51
52
53
54
55
56
57
58
59
60

Confocal Microscopy to Assess Gel Patterning

Confocal laser scanning microscopy was utilized to qualitatively assess the micropatterning process and to determine the dimensions of the microwells. PEG hydrogels were stained by covalently immobilizing FITC-conjugated BSA. BSA was pre-reacted for 30 min at room temperature with a 10-fold molar excess of a heterofunctional NHS-PEG-VS PEG linker (Nektar, Huntsville, AL, USA). The PEGylated protein was mixed with the precursors solution to graft at the termini of the thiolated PEG macromer. Images were acquired using a Leica DMR XA2 motorized upright confocal laser scanning microscope (Leica, Germany). Typically, z-stacks were acquired with a constant slice thickness of 3 μm , reconstructing a cross section profile of approx. 150 μm . Cross section analysis and image processing were done using Imaris 6.0 software.

Isolation of Neural Stem/Progenitor Cells

Epidermal growth factor (EGF)-dependent neurospheres cultures were generated from subventricular regions of postnatal (young adult; 1 month old) Hes5-GFP transgenic mice as previously described¹⁹. Briefly, subventricular regions were dissociated in 300 μL 1 : 1

1 Cordey et al.

2
3 papain : ovomucoid mix at 37 °C for 45 min. Papain mix: 30 U/ μ L papain (Sigma), 240
4
5 μ g/mL cysteine, 40 μ g/mL DNase, in L15 (Invitrogen); ovomucoid mix: 1.125 mg/mL
6
7 Trypsin inhibitor (Sigma), 0.5 mg/mL bovine serum albumin (BSA; Sigma), 40 ng/mL
8
9 DNA, in L15. The cells in the resulting cell suspension was centrifuged (5 min. 80g),
10
11 dissociated, resuspended and cultured in suspension in neurosphere medium (DMEM/F12
12
13 + Glutamax, Invitrogen) containing 10 ng/mL EGF (Peprotech), and 1 x B27 supplement
14
15 (Invitrogen) for 4 days at 37°C. The supernatant was then transferred to new flasks
16
17 containing fresh medium and the cells were allowed to grow in suspension for an
18
19 additional 2 days. Neurospheres were passaged with 0.25% trypsin in Versene
20
21 (Invitrogen) followed by mild mechanical trituration with a fire-polished pasteur pipette
22
23 and expanded at least twice before being seeded onto hydrogel microwell arrays in a 1 : 1
24
25 solutions comprising of fresh neurosphere medium and neurosphere conditioned
26
27 medium²⁰.
28
29
30
31
32
33
34
35
36

37 **Time-lapse Analyses of NSC Migration, Proliferation and Neurosphere Growth**

38
39 Glass slides patterned with hydrogel microwell arrays were fitted with the top of a Lab-
40
41 Tek II chamber (NUNC) and sealed with Elastosil silicone glue (Wacker Chemie AG,
42
43 Germany). Dissociated cells from neurosphere cultures (passage 2 to 4) were randomly
44
45 distributed and trapped in microwells by gravitational sedimentation at a density of 1.25 x
46
47 10⁴ cells/mL (corresponding to 2000 cells/96-well-sized pattern). For automated cell
48
49 culture, the slides were placed in the environmental chamber of an inverted microscope
50
51 (Zeiss, Axio Observer.Z1) equipped with a motorized Zeiss scanning stage. The XYZ
52
53 stage was programmed to repeatedly scan across the microwell array surface in a mosaic
54
55
56
57
58
59
60

1
2
3 pattern, acquiring phase contrast images at 10X magnification in defined time intervals
4
5 for a period of up to 4 days, or as specified. The resulting images were then automatically
6
7 compiled into a stack using the Metamorph software (Molecular Devices, USA).
8
9

10
11 Microwells containing a single live cell at time point $t = 0$ were followed over time by
12
13 visual inspection. Cells were scored as dead when they completely ceased to move and
14
15 markedly shrunk in size on the microwell surface. Cell death was confirmed via
16
17 fluorescence microscopy using Propidium Iodide (PI) staining (see [Supplementary Figure](#)
18
19 [1](#)). PI intercalates into double-stranded nucleic acids. It is excluded by viable cells but
20
21 can penetrate cell membranes of dying or dead cells. PI was added at a concentration of
22
23 1:1000 to the medium and time-lapse experiments were conducted in bright field and
24
25 fluorescence every four hours for a period of three days. Individual cell proliferation
26
27 kinetics were determined by manually scoring the number of cells per microwell at each
28
29 time point. The raw data containing the cell count and the region location was then
30
31 compiled on an Excel spreadsheet for further statistical analysis of the growth kinetics of
32
33 individual live cells.
34
35

36
37
38 Neurosphere areas were measured in phase contrast images using Metamorph software
39
40 (region of interest tool) and data was logged in an Excel sheet. Nuclei counterstained
41
42 with DAPI were then counted in the fluorescent image and added to the log sheet.
43
44

45
46 Migration analysis of Metamorph stacks was performed using an Image J plugin
47
48 (http://rsb.info.nih/ij/plugins/download/MultiTracker_.java). The coordinates of a cell's centroid in
49
50 each time frame were used to define its migration path. The paths were represented
51
52 graphically by overlaying multiple cell migration paths starting at the origin.
53
54
55
56
57
58
59
60

1
2
3
4
5
6
7
8
9
10
11
12
13
14
15
16
17
18
19
20
21
22
23
24
25
26
27
28
29
30
31
32
33
34
35
36
37
38
39
40
41
42
43
44
45
46
47
48
49
50
51
52
53
54
55
56
57
58
59
60

Cordey et al.

Retrospective ‘Phenotyping’ by Immunostaining

Cells grown on the arrays were fixed in 4% paraformaldehyde in phosphate-buffered saline (PBS, pH 7.4), washed in glycine buffer (0.1 M Glycine in PBS), permeabilized and blocked with 0.4% saponin, 4 % BSA in PBS and incubated overnight at 4°C in blocking solution containing a combination of the following primary antibodies: mouse anti-nestin (1:500; BD Biosciences), rabbit anti-GFAP (1:500; Dako), rabbit anti- β -TubulinIII (Tuj1; 1:250; Abcam), and mouse anti-O4 (1:500; R&D). Arrays were washed 3 x 30 min in glycine buffer and incubated for 2 h at room temperature with secondary antibodies anti-mouse Alexa 555 and anti-rabbit Alexa 647 (1:500; Invitrogen). Arrays were washed 3 x 30 min with glycine buffer, with 10 μ g/mL DAPI (Sigma) in the second wash. Arrays were stored at 4°C in PBS until visualized using an upright Leica TCS-SP2 AOBS confocal microscope with a 63x water immersion objective. Images were processed using deconvolution software Huygens 2.8 and reconstructed using Imaris 6.0 software.

Statistics

Data were analyzed statistically by ANOVA followed by pairwise comparisons using Fisher’s LSD test. Significance was set at $p < 0.05$.

RESULTS

Formation of PEG Hydrogel Microwell Arrays for NSC Culture

To address some of the complexities associated with the conventional neurosphere assay^{3-5, 7, 8}, we developed a novel family of arrayed microwell surfaces. We chose poly(ethylene glycol)-(PEG)-based hydrogels as substrates for single NSC culture for two reasons: *i*) these materials contain 95-98% water and as a result are very soft (*i.e.* an elastic modulus of a few hundred Pascal¹⁷); NSC would be exposed to an environment that to some extent recapitulates the biophysical characteristics of their *in vivo* niche, and *ii*) their extensive hydrophilicity renders the gels inert to protein adsorption and cell adhesion. As neurosphere growth occurs in suspension in the absence of cell adhesion², a topographically patterned gel surface could therefore readily trap cells to confined areas as they are not able to migrate in the absence of adhesion.

Adapting a previously developed cross-linking chemistry¹⁷, we fabricated microwell arrays from vinylsulfone- and thiol-terminated multifunctional PEG macromers **in a multi-step soft lithography process using poly(dimethylsiloxane) (PDMS) stamps (Fig. 1A)**. Each stamp (8 per film) consisted in squares corresponding to the area of a standard 96-well comprising ca. 1'000 wells with a diameter of 100 μm , a depth of 50 μm , and a well-to-well spacing of 50 μm . Confocal laser microscopy revealed a regular pattern of **hydrogel microwells with only slightly changed dimensions upon swelling (Fig. 1B and 1C)**. Notably, gels that were completely cross-linked before initiating the stamping process resulted in patterned microwells with a negligible depth of only 4.4 +/- 0.4 μm .

Cordey et al.

Live Imaging of NSC Cultures: Increasing the Sensitivity and Throughput of the Neurosphere Assay

Time-lapse microscopy was used to monitor NSC growth. The established *in vitro* method to study the behavior of these cells at the single cell level is to plate them at clonal density (100 cells/cm^2) in standard multi-well plastic culture plates (hereafter referred to as ‘plastic’), which we chose as the control treatment. Dissociated NSCs from suspension cultures were seeded on microwells at a density of $1.25 \times 10^4 \text{ cells/mL}$, which resulted in the majority of single wells being occupied by single cells. After 1 – 2 hours the cells had settled to the bottom of microwells and time-lapse experiments were started, imaging every 4 hours for 72 hours. The possibility to geographically confine cells was crucial for their efficient tracking (**Fig. 2**). Cells on plastic were extremely motile (**Fig. 2A** and **Supplementary Movie 1**), despite the lack of any adhesive cues in the serum-free medium. In approximately 15% of cases, cells left the field of view during the experiment. In marked contrast, cells cultured on PEG microwell arrays remained trapped and could easily be monitored over time (**Fig. 2B** and **Supplementary Movie 2**). Indeed, an automated analysis of migration paths of NSCs grown on these substrates confirmed this visual assessment (**Fig. 2C** and **D**). Therefore, trapping individual cells in hydrogel microwell arrays allows to study multiple, single, trapped cells in one field of interest (up to 24 microwells at 10X magnification). This dramatically increases the sensitivity and throughput of single NSC cultures. Neurosphere merging, which can occur in conventional suspension cultures of NSCs⁵, may also occur on PEG microwell arrays but only in cases where two or more cells settle within one microwell. However, at the seeding densities we selected, only a few microwells contained two or more cells, and

these events were easily excluded in subsequent image analysis.

Increased Viability of Single NSCs Cultured in Hydrogel Microwells

We next assessed the fate of individual stem cells of the population on the microwell array surface compared to plastic. Time-lapse movies of three independent experiments were visually inspected and wells containing single cells at time zero were tracked over time to distinguish between cell death, proliferation, or absence of cell divisions over the 3-day period (**Fig. 3A, Supplementary Movie 3**). Cell death was defined as complete loss of movement and extensive shrinking - a visual read-out that was verified using Propidium Iodide (PI) staining (see [Supplementary Figure 1](#)). Distinguishing these different fates, on PEG microwells we scored 31% +/- 3 of the population of single cells as dead, 20% +/- 8 as non-dividing, and the remaining 49% +/- 8 as proliferating cells that formed neurospheres of different sizes (see **Fig. 5**). Notably, viability of single cells decreased markedly within the first 24 hours and then leveled off (**Fig. 3B**). Death of single cells exposed to plastic occurred in 69 +/- 6% of cases, more than twice as frequently as on PEG (33 +/- 5%) (**Fig. 3C**).

NSC Proliferation and Neurosphere Formation Efficiency

The conventional neurosphere assay captures rapidly proliferating, sphere-forming cells that are believed to be primarily stem cells. This assumption has recently come under scrutiny^{4, 8}. We tried to assess the proliferation dynamics of individual neurosphere-derived cells in an unbiased fashion, independent of their growth behavior. We first scored the number of cells per microwell up to day 3, when divisions and cell numbers

1 Cordey et al.

2
3 could still be reliably assessed (**Fig. 4A**, top panel). We detected a heterogeneous
4
5 distribution of the time to the 1st division and the time for the 2nd cell cycle. The average
6
7 time to the 1st division of the entire population of single cells was ca. 18 hours.
8
9

10 Interestingly, three sub-populations were apparent (indicated by dashed lines), with 90%
11
12 of the cells dividing within the first 30 hours. The distribution of the 2nd cell cycle times
13
14 showed a slight shift towards longer times (population average: 25 hours). In particular,
15
16 30% of single cells divided a second time within the next 48 hours. To assess synchrony
17
18 in cell divisions kinetics, we quantified the time gap (Δt) between daughter cell divisions
19
20 of the second generation (**Fig. 4B**, scheme). Notably, 90% of all dividing cells showed
21
22 asynchronous divisions, defined as a Δt larger than 4 hours (**Fig. 4B**, right panel),
23
24 suggesting a different identity of the two progeny of the founding cell. After 72 hours in
25
26 culture, approximately 20% of the surviving single cells did not divide, while more than
27
28 30% divided **at least** once (**Fig. 4C**). In 20% of cases, one of the daughter cells divided a
29
30 second time resulting in three cells per well. The remaining 30% could be considered as
31
32 more proliferative, yielding 4 or more cells over the 3 days in culture.
33
34
35
36
37
38

39 To assess neurosphere-forming efficiency of the entire NSC population at the
40
41 endpoint of the experiment (*i.e.* 7 days), the number of spheres with a diameter $\geq 20 \mu\text{m}$ -
42
43 the threshold above which we defined cell clusters as neurospheres **assuming that they**
44
45 **had a diameter of at least 2 single cell diameters (measured as $\sim 10 \mu\text{m}$)** - on one array was
46
47 scored and compared to the number of wells occupied by cells that did not proliferate to
48
49 reach the size of a sphere. We found that approximately 30% of wells contained cells that
50
51 had proliferated to form a sphere, while ca. 70% of the wells contained single cells or
52
53 small aggregates of cells below 20 μm in diameter (not shown). Next, the area of
54
55
56
57
58
59
60

individual neurospheres was quantified via automated image analysis (**Fig. 5A**), revealing that half of the spheres had a diameter between 20 and 40 μm , 40% had a diameter between 40 and 60 μm , and less than 5% of all neurospheres grew to a size to fill out most of the microwell surfaces. To retrospectively correlate neurosphere diameters with cell numbers, we visualized the nuclei with DAPI after fixation, imaged and counted the cells (**Fig. 5B**). A good correlation was found between the number of nuclei/well and the surface area of the spheres ($R^2 = 0.9$). This correlation was used to plot a size histogram for the entire neurosphere population (**Fig. 5C**), binning sphere sizes according to categories of 10 cells. After 7 days of culture, the majority of neurospheres (ca. 60%) on the array were small, comprising less than 20 cells (referred to as NS type I), while only 5% of the population comprised large NS of 50 and more cells (NS type III). The remaining 35% was of intermediate size of 20-50 cells (NS type II). **Due to the likelihood of extensive neurosphere merging on flat plastic dishes, smaller neurospheres of type I or II that in our hands encompass the largest proportion of the population, can not be reliably detected. Not surprisingly, conventional read-outs of the neurosphere assay are biased towards rapidly growing clones, which may not necessarily be the stem cells. The microwell confinement in conjunction with time-lapse analyses allowed probing the dynamic behavior of large numbers of individual cells completely independent of their proliferation kinetics, and thus revealed the heterogeneity in cell fate and proliferation kinetics of a given cell population.**

Retrospective Phenotyping

Apart from the proliferation kinetics, the presence of phenotypic markers can be an

1 Cordey et al.

2
3 additional indicator correlating with stem cell function. We chose cells originating from
4 transgenic reporter mice expressing eGFP under the control of the Hes-5 promoter, a
5 downstream effector of Notch signaling¹⁹, to be able to probe stem cell phenotypes *in*
6 *situ*. That is, in these mice, GFP expression was shown to be restricted to multipotent
7 stem and progenitor cells of the developing embryonic brain¹⁹, and the expression of
8 Hes5-GFP has been reported to remain in the neurogenic regions of the postnatal and
9 adult brain (Basak, O. and Taylor, V., unpublished observations). In cells fixed after a 3-
10 day culture period on the microwell arrays, GFP+ cells accounted for ca. 30% of all cells
11 (single or part of a sphere) as assessed with confocal microscopy (**Fig. 6A, B** and
12 **Supplementary Movie 4**). Dissociated cells from standard suspension neurosphere
13 cultures (passage 2 to 5) analyzed by FACS also contained on average 30% of GFP+
14 cells (data not shown). More than 90% of the cells strongly expressed Nestin (**Fig. 6B**;
15 Nestin marked in red), a filament marker of neural progenitors. The Nestin+ cells were
16 observed to preferentially be located in direct contact with the hydrogel surface. We
17 could not detect any GFAP or β -Tubulin III-positive cells after three days, suggesting
18 that the cells had not differentiated at this time-point.

19
20
21
22
23
24
25
26
27
28
29
30
31
32
33
34
35
36
37
38
39
40
41 Neurospheres developed from single cells on the array during 7 days were
42 comprised of cells with phenotypes of both stem/progenitor cells and differentiated cells
43 (**Fig. 6C, D** and **Supplementary Movie 5**). We detected Hes5-GFP-positive and Nestin-
44 positive cells alongside a substantial number of GFAP-positive cells (**Fig. 6C**;
45 Nestin=red, GFAP=yellow). Nestin+ cells appeared to be located in the periphery of the
46 neurosphere, while GFAP+ cells were found in the center and in contact with the
47 surface²⁰. Image analysis on several confocal sections revealed that GFAP and Nestin
48
49
50
51
52
53
54
55
56
57
58
59
60

1
2
3 staining did not colocalize (data not shown), consistent with previous results showing
4
5 neurospheres contain cells that start expressing GFAP after 5 days in culture¹⁹.
6
7
8
9

10 11 12 **DISCUSSION**

13
14
15 The neurosphere assay is a versatile tool in NSC biology. It has helped to expand putative
16
17 stem/progenitor cells, to assess their self-renewal capability and multipotency, and to
18
19 shed light on the role of mechanisms that regulate NSC-like cells³. Similar sphere-
20
21 forming assays are used in a wealth of other stem cell systems including skin²¹, breast²²,
22
23 or pancreas²³, and even in the context of cancer stem cells²⁴. Given its significance, it
24
25 goes without saying that such cytosphere assays must function efficiently, particularly
26
27 with regards to their clonality. This is often not the case, except where single cells are
28
29 seeded in single wells, which renders the assay highly inefficient. The hydrogel
30
31 microwell platform introduced here addresses some of the limitations of the standard
32
33 neurosphere assay.
34
35
36
37

38
39 As we have demonstrated by tracking single cell migration, the possibility of
40
41 geographically restricting cells not only dramatically simplifies live-cell imaging
42
43 capability, but also eliminates merging events that appear to be a bottleneck of the
44
45 standard assay^{5, 6}. While cell trapping and high-throughput single cell experimentation is
46
47 afforded by several other microwell array systems previously developed for cell culture²⁵⁻
48
49 ²⁸, in contrast to PDMS or glass substrates that are predominantly used for that purpose,
50
51 the biomimetic properties of our platform and its implications described below, may be a
52
53 beneficial hallmark of hydrogel-based arrays^{29, 30}.
54
55
56
57
58
59
60

Cordey et al.

Indeed, this novel platform appears to provide a microenvironment that greatly enhances single cell viability compared to plastic (**Fig. 3**), allowing the study of a much higher proportion of single cells from a given NSC population than currently possible. Death can occur at multiple stages of the culture phase, before or after cell divisions (i.e. in the forming neurosphere). **In the latter case it may be related to apoptosis as a regulatory mechanism of cell numbers. We rarely detected single, non-dividing (viable) cells on plastic, which may be due to the rapid merging of single cells with motile neurospheres but perhaps is also due to preferential death of individual cells on this substrate. Strikingly, on PEG hydrogels, of the 70% of surviving single cells approximately 20% never divide. We believe that the soft and hydrated environment provided by PEG gels, reminiscent of the *in vivo* extracellular milieu, may explain this enhanced single cell viability. Indeed, it has been reported that the elasticity of a substrate itself may affect viability and stem cell fate directly, implying involvement of mechanotransduction mechanisms³¹. However, for this to play a role one would expect cell adhesion to be a prerequisite, transmitting forces from the outside to the inside of the cell via receptor-ligand interactions, a phenomenon which may not play an important role in the case of the non-adherent neurospheres. On the other hand, it is conceivable that the high water content of the substrate enhances diffusion of nutrients and morphogens to the cells, which can occur from all sides in the case of hydrogels. The underlying mechanisms responsible of increased viability warrants further investigation.**

We detected non-dividing cells alongside three types of neurospheres on the array that differ dramatically in size (**Fig. 5C**): small type I spheres which made up 60% of the population, intermediate sizes of type II (35%), and large spheres of type III (5%).

1
2
3 Follow-up studies should dissect the phenotype, self-renewal function and multipotency
4 of the non-dividing cells and of the three types of neurospheres we have identified using
5 the novel array-format. For example, if subjected to an environment that favors
6 differentiation, it would be possible to address whether cells with different proliferation
7 behaviors generate different cell-types and thus may represent defined NSC lineages, and
8 whether there is there a link between neurosphere size and multipotentiality. We believe
9 that the microwell arrays presented here represent an ideal platform to address these
10 questions, and that they may help, if combined with *in vivo* stem cell transplantation
11 studies, to bring us closer to a better understanding of stem cell biology.
12
13
14
15
16
17
18
19
20
21
22
23
24
25
26
27
28

29 **ACKNOWLEDGMENTS**

30
31 We thank our collaborators Yunsuk Jo for help with PEG syntheses, Steffen Cosson for
32 single cell migration analysis, Andhyk Halim for help with scoring, Adrian Ranga for
33 critical reading of the manuscript, J-C Floyd Sarria and Thierry Laroche of the
34 Bioimaging and Optics platform (EPFL) for help with image acquisition and analysis.
35
36 This work was supported by the SNSF grant FN 205321-112323/1 and by a EURYI
37
38
39
40
41
42
43
44
45
46
47
48
49
50
51
52
53
54
55
56
57
58
59
60
award to M.P.L.

Cordey et al.

References

1. Bryder D, Rossi DJ, Weissman IL. Hematopoietic stem cells - The paradigmatic tissue-specific stem cell. *American Journal of Pathology*. 2006;169:338-346.
2. Reynolds BA, Weiss S. Generation of Neurons and Astrocytes from Isolated Cells of the Adult Mammalian Central-Nervous-System. *Science*. 1992;255:1707-1710.
3. Singec I, Quinones-Hinojosa A. Neurospheres. In: Gage FH, Kempermann G, Song H, eds. *Adult Neurogenesis*. Cold Spring Harbor, New York: Cold Spring Harbor Laboratory Press; 2007:119-134.
4. Reynolds BA, Rietze RL. Neural stem cells and neurospheres - re-evaluating the relationship. *Nature Methods*. 2005;2:333-336.
5. Singec I, Knoth R, Meyer RP, et al. Defining the actual sensitivity and specificity of the neurosphere assay in stem cell biology. *Nature Methods*. 2006;3:801-806.
6. Jessberger S, Clemenson GD, Gage FH. Spontaneous fusion and nonclonal growth of adult neural stem cells. *Stem Cells*. 2007;25:871-874.
7. Deleyrolle LP, Rietze RL, Reynolds BA. The neurosphere assay, a method under scrutiny. *Acta Neuropsychiatrica*. 2008;20:2-8.
8. Louis SA, Rietze RL, Deleyrolle LP, et al. Enumeration of neural stem and progenitor cells in the neural colony forming cell assay. *Stem Cells*. 2008;DOI: 10.1634/stemcells.2007-0867.
9. Tropepe V, Sibilina M, Ciruna BG, et al. Distinct neural stem cells proliferate in response to EGF and FGF in the developing mouse telencephalon. *Developmental Biology*. 1999;208:166-188.
10. Passegue E, Wagers AJ, Giuriato S, et al. Global analysis of proliferation and cell cycle gene expression in the regulation of hematopoietic stem and progenitor cell fates. *Journal of Experimental Medicine*. 2005;202:1599-1611.
11. Nygren JM, Bryder D, Jacobsen SEW. Prolonged cell cycle transit is a defining and developmentally conserved hemopoietic stem cell property. *Journal of Immunology*. 2006;177:201-208.
12. Young JC, Varma A, DiGiusto D, et al. Retention of quiescent hematopoietic cells with high proliferative potential during ex vivo stem cell culture. *Blood*. 1996;87:545-556.
13. Falconnet D, Csucs G, Grandin HM, et al. Surface engineering approaches to micropattern surfaces for cell-based assays. *Biomaterials*. 2006;27:3044-3063.
14. Khademhosseini A, Langer R, Borenstein J, et al. Microscale technologies for tissue engineering and biology. *Proceedings of the National Academy of Sciences of the United States of America*. 2006;103:2480-2487.
15. Underhill GH, Bhatia SN. High-throughput analysis of signals regulating stem cell fate and function. *Current Opinion in Chemical Biology*. 2007;11:357-366.
16. Lutolf MP, Hubbell JA. Synthetic biomaterials as instructive extracellular microenvironments for morphogenesis in tissue engineering. *Nat Biotechnol*. 2005;23:47-55.
17. Lutolf MP, Hubbell JA. Synthesis and physicochemical characterization of end-linked poly(ethylene glycol)-co-peptide hydrogels formed by Michael-type addition. *Biomacromolecules*. 2003;4:713-722.
18. Huang L, Nair PK, Nair MTS, et al. Chemical deposition of Bi₂S₃ thin films on glass substrates pretreated with organosilanes. *Thin Solid Films*. 1995;268:49-56.
19. Basak O, Taylor V. Identification of self-replicating multipotent progenitors in the embryonic nervous system by high Notch activity and Hes5 expression. *European Journal of Neuroscience*. 2007;25:1006-1022.
20. Nyfeler Y, Kirch RD, Mantei N, et al. Jagged1 signals in the postnatal subventricular zone are required for neural stem cell self-renewal. *Embo J*. 2005;24:3504-3515.
21. Toma JG, Akhavan M, Fernandes KJL, et al. Isolation of multipotent adult stem cells from the dermis of mammalian skin. *Nature Cell Biology*. 2001;3:778-784.
22. Matsuda M, Imaoka T, Vomachka AJ, et al. Serotonin regulates mammary gland development via an autocrine-paracrine loop. *Developmental Cell*. 2004;6:193-203.

Microarrayed Neurosphere Culture

- 1
 - 2
 - 3
 - 4
 - 5
 - 6
 - 7
 - 8
 - 9
 - 10
 - 11
 - 12
 - 13
 - 14
 - 15
 - 16
 - 17
 - 18
 - 19
 - 20
 - 21
 - 22
 - 23
 - 24
 - 25
 - 26
 - 27
 - 28
 - 29
 - 30
 - 31
 - 32
 - 33
 - 34
 - 35
 - 36
 - 37
 - 38
 - 39
 - 40
 - 41
 - 42
 - 43
 - 44
 - 45
 - 46
 - 47
 - 48
 - 49
 - 50
 - 51
 - 52
 - 53
 - 54
 - 55
 - 56
 - 57
 - 58
 - 59
 - 60
23. Seaberg RM, Smukler SR, Kieffer TJ, et al. Clonal identification of multipotent precursors from adult mouse pancreas that generate neural and pancreatic lineages. *Nature Biotechnology*. 2004;22:1115-1124.
24. Hemmati HD, Nakano I, Lazareff JA, et al. Cancerous stem cells can arise from pediatric brain tumors. *Proceedings of the National Academy of Sciences of the United States of America*. 2003;100:15178-15183.
25. Revzin A, Tompkins RG, Toner M. Surface engineering with poly(ethylene glycol) photolithography to create high-density cell arrays on glass. *Langmuir*. 2003;19:9855-9862.
26. Chin VI, Taupin P, Sanga S, et al. Microfabricated platform for studying stem cell fates. *Biotechnology and Bioengineering*. 2004;88:399-415.
27. Dusseiller MR, Schlaepfer D, Koch M, et al. An inverted microcontact printing method on topographically structured polystyrene chips for arrayed micro-3-D culturing of single cells. *Biomaterials*. 2005;26:5917-5925.
28. Mohr JC, de Pablo JJ, Palecek SP. 3-D microwell culture of human embryonic stem cells. *Biomaterials*. 2006;27:6032-6042.
29. Karp JM, Yeh J, Eng G, et al. Controlling size, shape and homogeneity of embryoid bodies using poly(ethylene glycol) microwells. *Lab on a Chip*. 2007;7:786-794.
30. Moeller HC, Mian MK, Shrivastava S, et al. A microwell array system for stem cell culture. *Biomaterials*. 2008;29:752-763.
31. Engler AJ, Sen S, Sweeney HL, et al. Matrix elasticity directs stem cell lineage specification. *Cell*. 2006;126:677-689.

1
2
3
4
5
6
7
8
9
10
11
12
13
14
15
16
17
18
19
20
21
22
23
24
25
26
27
28
29
30
31
32
33
34
35
36
37
38
39
40
41
42
43
44
45
46
47
48
49
50
51
52
53
54
55
56
57
58
59
60

Cordey et al.

Figure Captions

Figure 1. Overview of multistep process to fabricate hydrogel microwell arrays for NSC culture. **(A)** Thin PEG hydrogel films of defined thickness are cast on a modified glass cover slide (step I). A PDMS stamp containing an array of micropillars fabricated from a micropatterned Silicon wafer is gently placed onto the PEG film to stamp the desired microwell array topography (step II). Microwell arrays are washed and sealed for subsequent stem cell culture (step III). Multiarm PEG macromers bearing thiol- and vinylsulfone end-groups serve as precursors of crosslinked polymer networks formed under mild conditions via conjugate addition reaction. **(B)** Hydrogel microwell arrays fabricated via stamping of PDMS templates. Micrographs from 3D-reconstructions of 3- μm confocal z-stacks reveal a regular pattern of microwells. **(C)** Obtained dimensions of individual microwells after 30 min of film formation (partial cross-linking) and swelling in water: $94.3 \pm 2.6 \mu\text{m}$ diameter and $39.6 \pm 2.4 \mu\text{m}$ depth. The cross-linking kinetics significantly influence microwell depth; for example, stamping after complete cross-linking led to patterns of only $4.4 \pm 0.4 \mu\text{m}$.

1
2
3
4
5
6
7
8
9
10
11
12
13
14
15
16
17
18
19
20
21
22
23
24
25
26
27
28
29
30
31
32
33
34
35
36
37
38
39
40
41
42
43
44
45
46
47
48
49
50
51
52
53
54
55
56
57
58
59
60

Figure 2. PEG microwells restrict migration of single NSCs. **(A)** Still images from a 3-day time-lapse movie showing extensive migration of a single NSC on an untreated standard 96-well plastic plate (BD Biosciences). Scale bar = 100 μm . **(B)** In marked contrast, in all cases and over extended culture periods, single NSCs on the bottom of PEG microwells remained trapped. **(C)** Representative migration paths of 10 individual NSCs overlaid at a common starting point on plastic (left panel) and in PEG microwells (right panel). Two out of 10 cells left the field of view, while cells on microwell arrays were constrained in their migration distance to the well dimensions. All tracks were acquired during an observation period of 72 hours. **(D)** The total average migration distance covered by single NSCs (left panel) and the average migration rate (right panel) on PEG microwells are significantly lower than on plastic. $**p < 0.01$.

Cordey et al.

1
2
3 **Figure 3.** Fate and viability of single NSCs cultured on PEG hydrogel microarray. (A)
4 Neural stem cells were trapped in microwells and imaged every 4 hours over a 72-hour
5
6 time period. Circles indicate wells that contained single cells at the time of seeding (t = 0
7
8 hrs), and color indicates the representative fate of these cells over 24, 48 and 72 hrs. **The**
9
10 **diameter of one microwell is ca. 95 μm .** (B) Single cell viability in microwells was
11
12 quantified by visually inspecting every frame of a time-lapse movie over the 3-day period
13
14 **and validated via PI staining (see [Supplementary Figure 1](#)).** (C) Single NSCs seeded at
15
16 ‘clonal’ density (i.e. 100 cells/cm²) on uncoated 96-well plastic culture plates had
17
18 significantly lower viability after 3 days than cells seeded on PEG hydrogel microwells
19
20 (***p* < 0.01). Data shown are mean \pm SD and cell viability is represented as a percentage
21
22 of the total number of single cells scored at time 0 (n = 3 independent experiments, > 80
23
24 single cells/experiment).
25
26
27
28
29
30
31
32
33
34
35
36
37
38
39
40
41
42
43
44
45
46
47
48
49
50
51
52
53
54
55
56
57
58
59
60

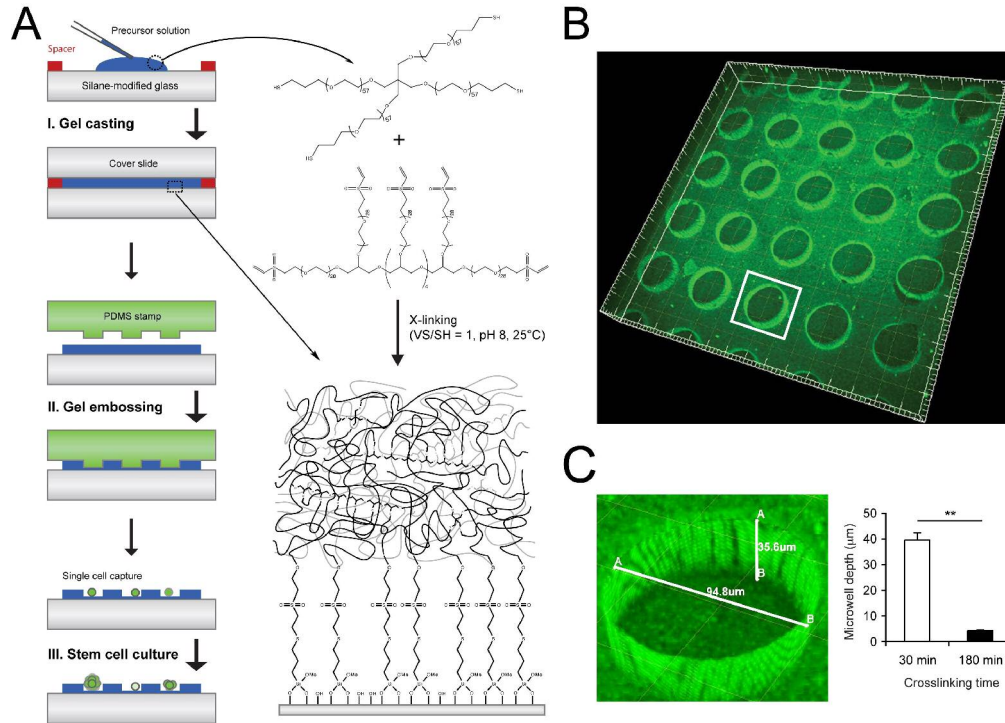
1
2
3
4 **Figure 4.** Quantification of initial single NSC proliferation kinetics on hydrogel
5
6 microwell arrays up to 3 days in culture. (A) Single NSCs trapped in microwells were
7
8 imaged by time-lapse microscopy and visually inspected to determine the distribution of
9
10 the time to the 1st, and the time between the 1st and 2nd division (n=140 cells/histogram
11
12 for 1st division, and n=77 for the 2nd division, respectively). Top panels show a
13
14 representative example of a cell dividing twice (arrowheads) to produce 3 daughter cells.
15
16 **The diameter of the microwell is ca. 95 μm .** (B) The time gap Δt between divisions of the
17
18 1st generation of daughter cells was chosen as a read-out for synchrony in division
19
20 behavior. A 4-hr threshold was chosen: synchronous: $\Delta t < 4\text{hr}$, asynchronous: $\Delta t > 4\text{hr}$. 90%
21
22 of the population of dividing cells showed asynchronous division kinetics. (C) Histogram
23
24 of cells per well generated after a 3-day culture period reveals a large heterogeneity in
25
26 neurosphere sizes (n = 3 independent experiments, > 80 single cells/experiment). Data
27
28 shown are mean \pm SD.
29
30
31
32
33
34
35
36
37
38
39
40
41
42
43
44
45
46
47
48
49
50
51
52
53
54
55
56
57
58
59
60

1 Cordey et al.

2
3 **Figure 5.** Quantification of single NSC proliferation kinetics on hydrogel microwell
4 arrays after 7 days in culture. (A) Histogram of neurosphere diameters generated after a
5 7-day culture period reveals a large heterogeneity in neurosphere sizes. Neurosphere were
6 counted and their area and diameter were measured via image analysis (Metamorph) from
7 bright field images. (B) The number of DAPI-stained nuclei was determined by image
8 analysis and correlated with the above neurosphere area. Right panels show an example
9 of DAPI-stained nuclei and the corresponding phase contrast images. **The diameter of**
10 **one microwell is ca. 95 μm .** (C) Spheres were categorized according to their size into
11 small (NS I), intermediate (NS II) and large spheres (NS III). Data shown are mean \pm SD
12 and population behavior is represented as a percentage of the total number of
13 neurospheres with a diameter $\geq 20 \mu\text{m}$ (total 127 NS scored on 4 different arrays).
14
15
16
17
18
19
20
21
22
23
24
25
26
27
28
29
30
31
32
33
34
35
36
37
38
39
40
41
42
43
44
45
46
47
48
49
50
51
52
53
54
55
56
57
58
59
60

1
2
3 **Figure 6.** Phenotype of neurosphere-forming cells. NSCs were grown on microwell
4
5 arrays, fixed after 3 or 7 days, respectively, and stained with Nestin, GFAP, O4, and β -
6
7 tubulin III for subsequent imaging via confocal microscopy. (A, B) Two sections of a 3-
8
9 day old sphere show Hes5-GFP-positive cells (=green), and Nestin-positive (=red) cells.
10
11 The other markers were not detected after 3 days. (C, D) Two sections of a 7-day old
12
13 sphere show Nestin-positive cells located at the periphery, with GFAP-positive cells
14
15 (=yellow) and GFP-positive cells in the center. O4 and β -tubulin III cells were not
16
17 detected. DAPI stain identifies cell nuclei (blue). Scale bar = 20 μ m.
18
19
20
21
22
23
24
25
26
27
28
29
30
31
32
33
34
35
36
37
38
39
40
41
42
43
44
45
46
47
48
49
50
51
52
53
54
55
56
57
58
59
60

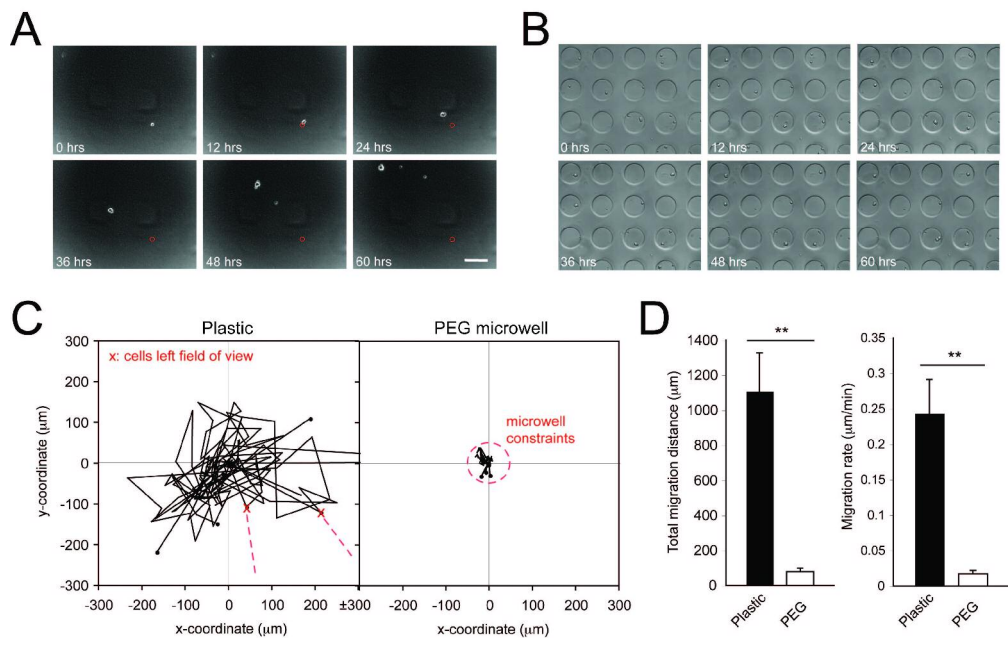
Cordey et al., Figure 1



253x199mm (300 x 300 DPI)

1
2
3
4
5
6
7
8
9
10
11
12
13
14
15
16
17
18
19
20
21
22
23
24
25
26
27
28
29
30
31
32
33
34
35
36
37
38
39
40
41
42
43
44
45
46
47
48
49
50
51
52
53
54
55
56
57
58
59
60

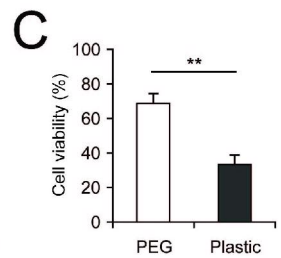
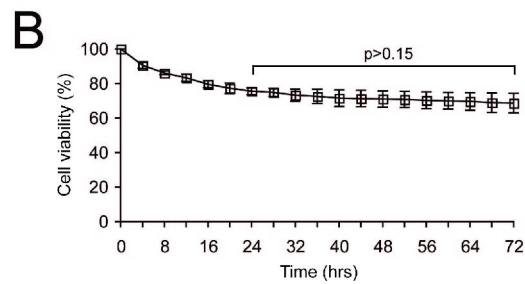
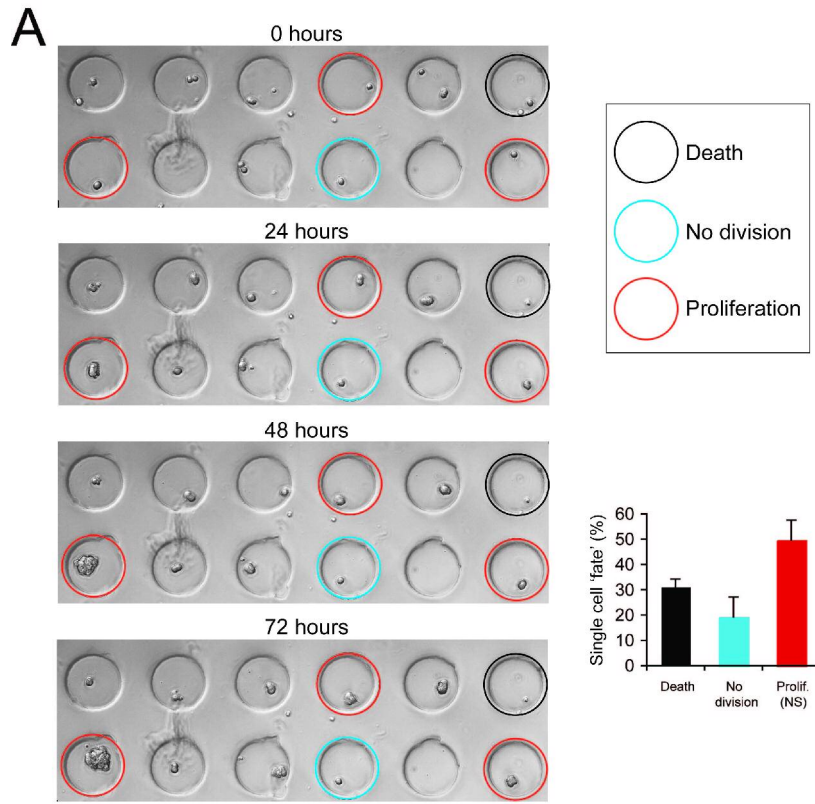
Cordey et al., Figure 2



1138x808mm (72 x 72 DPI)

review

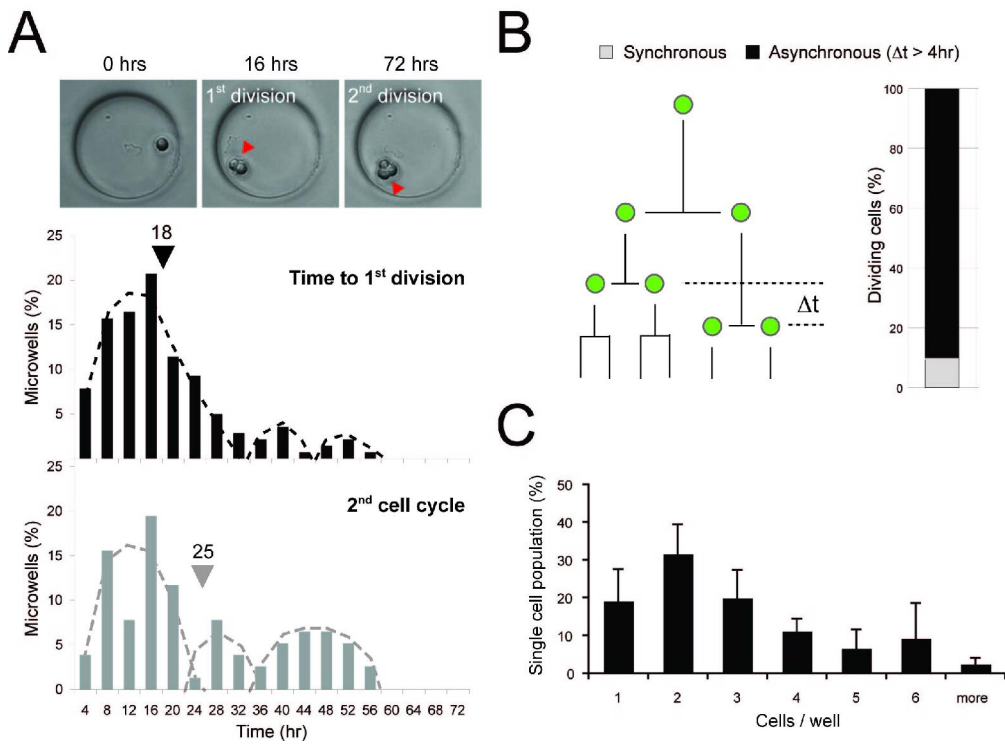
Cordey et al., Figure 3



742x1101mm (72 x 72 DPI)

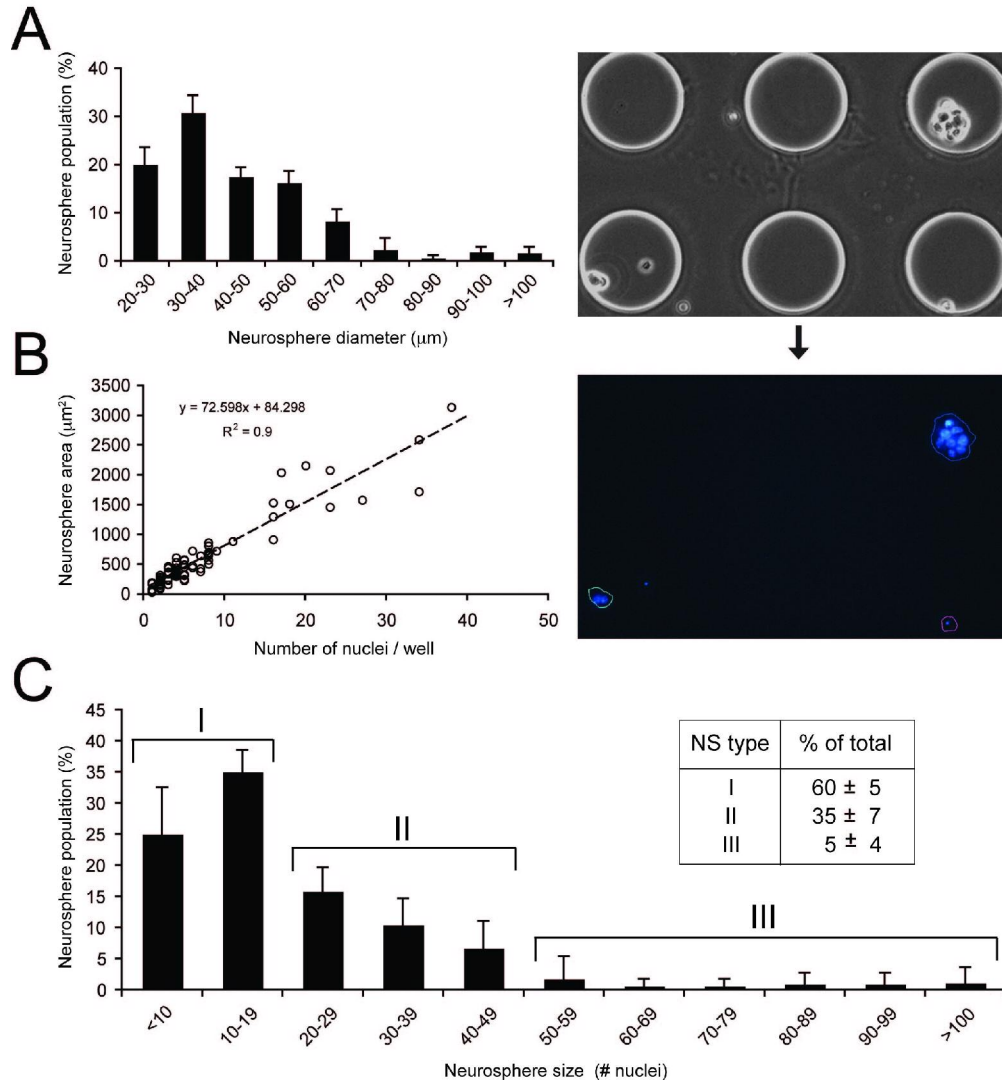
1
2
3
4
5
6
7
8
9
10
11
12
13
14
15
16
17
18
19
20
21
22
23
24
25
26
27
28
29
30
31
32
33
34
35
36
37
38
39
40
41
42
43
44
45
46
47
48
49
50
51
52
53
54
55
56
57
58
59
60

Cordey et al., Figure 4



745x644mm (72 x 72 DPI)

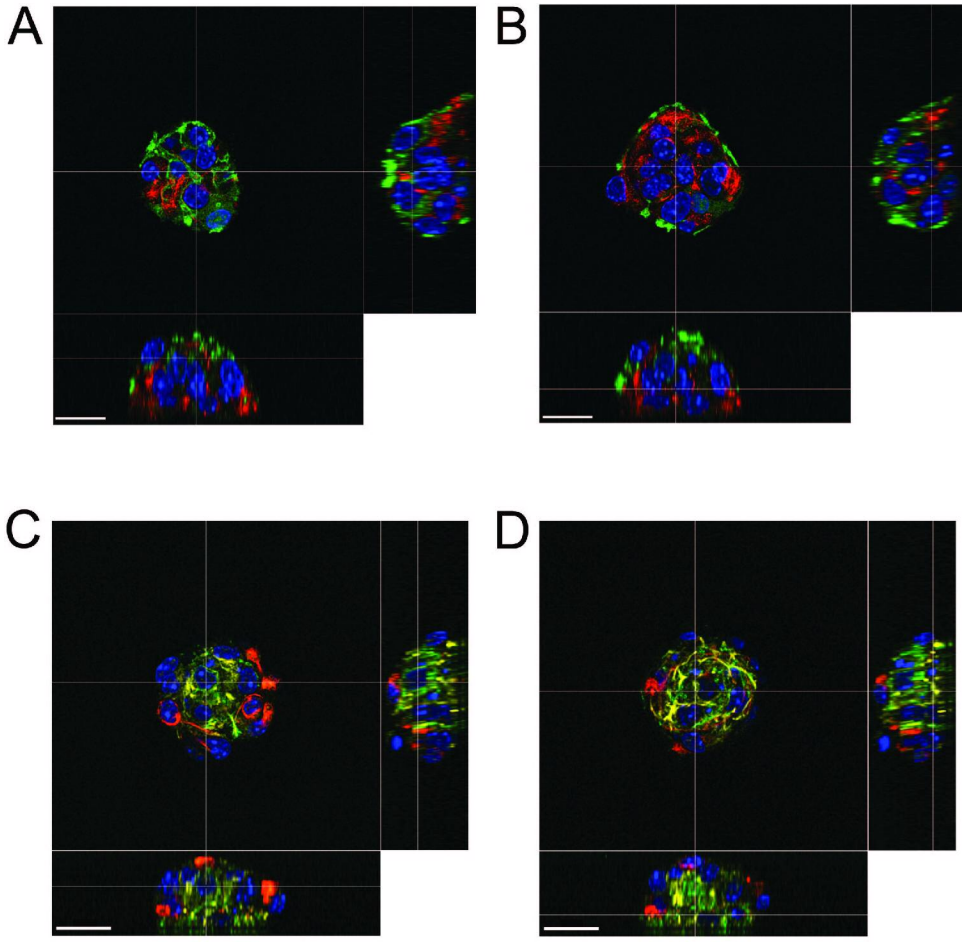
Cordey et al., Figure 5



721x863mm (72 x 72 DPI)

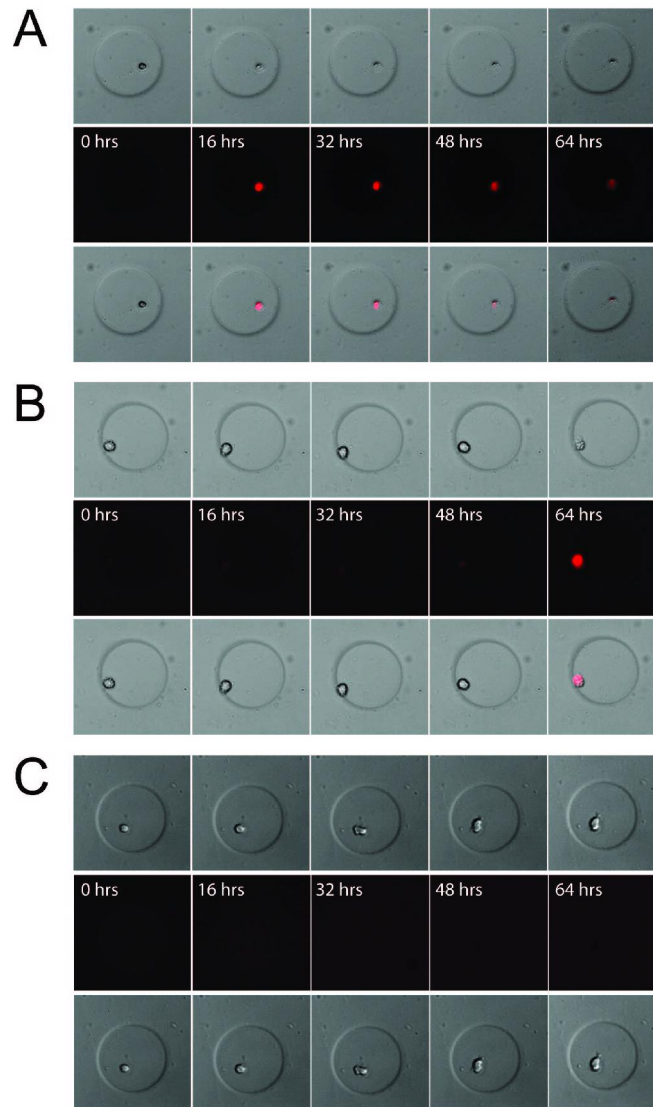
1
2
3
4
5
6
7
8
9
10
11
12
13
14
15
16
17
18
19
20
21
22
23
24
25
26
27
28
29
30
31
32
33
34
35
36
37
38
39
40
41
42
43
44
45
46
47
48
49
50
51
52
53
54
55
56
57
58
59
60

Cordey et al., Figure 6



786x984mm (72 x 72 DPI)

Cordey et al., Supplementary Figure 1



612x1124mm (72 x 72 DPI)

Supplementary Figure 1, Cordey *et al.*

Representative examples of still images from fluorescent time-lapse experiments to assess cell viability and time-points of cell death via Propidium Iodide (PI) staining. Images were acquired in bright field and fluorescence every 4 hour for a period of 72 hrs. (A and B) PI effectively marks dying and dead cells. Cell death is also readily apparent by a complete loss of cell movement and extensive shrinking in size. Cell death occurred at different time-points of the experiment, as quantified in **Figure 3B** of the manuscript. Top panels: bright field images, middle panels: fluorescent images, bottom panels: overlays of both. (C, control) Viable cells are negative for PI over the entire course of the experiment.

Supplementary Video legends, Cordey *et al.*

Supplementary Video 1

Representative time-lapse video microscopy demonstrating extensive migrating behavior of a single neurosphere-forming cell on an uncoated, standard plastic 96-well plate. Dissociated neurosphere cultures derived from adult mice subventricular zone were seeded at clonal density (100 cells/cm²) in 96-well plates placed in the environmental chamber of an inverted microscope (Zeiss, Axio Observer.Z1), and imaged every 30 min for 64 hours. Note how the motile cell divides and leaves behind cells (or cell fragments) on its path, until it leaves the field of view. Cellular processes allowing motility can be better appreciated at higher magnification in Supplementary Video 3.

Supplementary Video 2

Representative time-lapse video microscopy showing isolation and geographical confinement of 7 single cells (blue circles) in PEG hydrogel microwells (microwell diameter = 100 μm). Dissociated neurosphere cultures derived from the subventricular zone of postnatal mice were seeded on PEG hydrogel microarrays and imaged every 4 hours for 80 hours. Note the different proliferative potential of the cells followed in the same field of view, which can be seen at higher magnification in Supplementary Video 3.

Supplementary Video 3

Higher magnification of a single neurosphere-forming cell trapped in a PEG microwell. Images were captured every 4 hours for 72 hours, showing how cell divisions could be scored over this time period. This magnification also reveals cellular processes permitting motility.

Supplementary Video 4

3D reconstruction of a neurosphere grown on PEG hydrogel microarrays for 3 days. Cells originated from transgenic reporter mice expressing eGFP under the control of Hes-5 promoter, a downstream effector of Notch signaling. Confocal images show Hes5-GFP (green) expression and neural stem cell marker nestin immunostaining (red), confirming the neural stem cell phenotype of these cells. Nuclei were counterstained with DAPI (blue). Images were acquired using a Leica DMR XA2 motorized upright confocal laser

1
2
3 scanning microscope. Z-stacks were acquired with a slice thickness of 1.2 μm ,
4 reconstructing a cross section profile of approximately 30 μm . Note that we did not detect
5 any GFAP, β -tubulin III or O4 staining, which would indicate astrocytic, neuronal or
6 oligodendrocytic differentiation.
7
8

9 Supplementary Video 5

10 3D reconstruction of a neurosphere grown on PEG hydrogel microarrays for 7 days.
11 Confocal images show that Hes5-GFP (green) and nestin (yellow) are still expressed,
12 with nestin-positive cells located at the edge of the sphere. Core cells show GFAP (red)
13 expression, a marker of astrocytic differentiation. Nuclei were counterstained with DAPI
14 (blue). Note that we did not detect any β -tubulin III or O4 staining, which would indicate
15 neuronal or oligodendrocytic differentiation.
16
17
18
19
20
21
22
23
24
25
26
27
28
29
30
31
32
33
34
35
36
37
38
39
40
41
42
43
44
45
46
47
48
49
50
51
52
53
54
55
56
57
58
59
60